Insight into the differences in carbon dots prepared from fish scales using conventional hydrothermal and microwave methods

Chengzhi Xu
Wuhan Polytechnic University
Xiao Xiao
Wuhan Polytechnic University
Chaonan Cai
Wuhan Polytechnic University
Qunpeng Cheng
Wuhan Polytechnic University
Lian Zhu
Wuhan Polytechnic University
Juntao Zhang
Wuhan Polytechnic University
Benmei Wei
Wuhan Polytechnic University
Haibo Wang (wanghaibo216@126.com)
Wuhan Polytechnic University

Research Article

Keywords: Fish Scales, Carbon Dots, Hydrothermal Method, Microwave Method

Posted Date: January 3rd, 2023

DOI: https://doi.org/10.21203/rs.3.rs-2344281/v1

Version of Record: A version of this preprint was published at Environmental Science and Pollution Research on March 7th, 2023. See the published version at https://doi.org/10.1007/s11356-023-26275-z.

Abstract

The preparation of carbon dots (CDs) from waste fish scales is an attractive and high-value transformation. In this study, fish scales were used as a precursor to prepare CDs, and the effects of hydrothermal and microwave methods on their fluorescence properties and structures were evaluated. The microwave method was more conducive to the self-doping of nitrogen due to rapid and uniform heating. However, the low temperature associated with the microwave method resulted in the insufficient dissolution of the organic matter in fish scales; thus, the organic matter was difficult to completely dehydrate and condense, but formed nanosheet-like CDs, whose emission behavior had no significant correlation with excitation. Although the CDs prepared using the conventional hydrothermal had a lower doping amount of N element, the relative pyrrolic N content was higher, which was beneficial in improving their quantum yield. Additionally, the controllable high temperature and sealed environment used for the conventional hydrothermal could promote the dehydration and condensation of the organic matter in fish scales to form CDs with a higher degree of carbonization, uniform size, and higher C = O/COOH content. CDs prepared using the conventional hydrothermal exhibited higher quantum yield and excitation wavelength-dependent emission behavior.

1 Introduction

In the past few decades, with a significant increase in the production of aquatic products worldwide, its consumption has also increased, and the amount of biological waste from fisheries has also continued to grow(Golden et al. 2021). The internal organs, heads, and scales of fish in biowaste have attracted increasing attention due to their low commercial value, the lack of effective high-value utilization methods, and the threat posed to human health and the environment. The rational use of fish scales, fish skin, fish bones, and other aquatic-processing wastes can not only promote the sustainable and healthy development of the aquatic-processing industry but also reduce environmental pollution.(Krishnani et al. 2022, Lee et al. 2022, Rodrigues et al. 2021, Sierra et al. 2021)

The main chemical components of fish scale waste include collagen and hydroxyapatite, which are rich in carbon, hydrogen, oxygen, and nitrogen. They constitute inexpensive and readily available nitrogenous biomass waste.(Deb et al. 2019, Luo et al. 2020, Niu et al. 2019) Among the many high-value conversion pathways, the use of fish scale waste as a starting material for the preparation of nitrogen-doped CDs has the characteristics of easy availability of precursors, simple reaction conditions, the high added value of the products, as well as good environmental protection and economic benefits.(Zhang et al. 2018) Hydrothermal method is the primary technique to prepare CDs from fish scales, and calcium phosphate by-products are usually formed. Ashraf et al. prepared four high-value nanoproducts including CDs using *Labeo rohita* scales as raw material and using the hydrothermal reaction.(Ashraf et al. 2021) Athinarayanan et al. treated *Lethrinus lentjan* scales at 280°C. Using hydrothermal treatment, the organic and inorganic substances in fish scales were converted into CDs and hydroxyapatite nanoparticles. A study of cytotoxicity behavior showed that the fish scale-derived materials were biocompatible and nontoxic and that they could be suitable for bioimaging and bone tissue engineering applications.

(Athinarayanan et al. 2020) Campalani et al. synthesized CDs from *Dicentrarchus labrax* scales using the hydrothermal method and applied them to photocatalytic reactions (photoreduction reactions of methyl viologen).(Campalani et al. 2021) Zhang et al. used *Crucian carp* scales as a precursor to prepare highly fluorescent CDs with nitrogen and oxygen functional groups by the hydrothermal reaction. The CDs exhibited strong fluorescence emission at 430 nm with a relative quantum yield of 6.9%, low cytotoxicity, strong fluorescence stability, and good ionic strength for photobleaching. Moreover, the fluorescence of these CDs could be efficiently and selectively quenched by Fe^{3+} ions, rendering the CDs suitable for use as fluorescent Fe^{3+} nanoprobes.(Zhang et al. 2019) Dhandapani et al. synthesized green-fluorescent hydrophilic CDs using the hydrothermal method where fish scales were used as raw material. (Dhandapani et al. 2020) In addition to the hydrothermal method, Yao et al. prepared CDs with blue fluorescence using ultrasonic physical peeling using waste *Ctenopharyngodon idella* scales as raw material, and applied them for the analysis and detection of Fe^{3+}.(Yao et al. 2020) Chen et al. pretreated whitefish scales and used it as a starting material; they carbonized the scales at 260 ℃ for 2 h in an atmosphere of purified nitrogen to obtain CDs with multicolor fluorescence.(Chen et al. 2016)

Microwave heating has attracted the attention of scientific researchers owing to its simultaneous, uniform, efficient, and rapid response, and short reaction time.(Ghanem et al. 2020, Sharma et al. 2017, Xin et al. 2022, Zhao et al. 2019) However, the differences in the structure and performance of CDs prepared using the conventional hydrothermal and microwave methods have not been reported. Therefore, it is important to compare the differences in the fluorescence performance and composition of CDs prepared using conventional hydrothermal and microwave methods. In this study, CDs were prepared from silver carp scales. Accordingly, the key process parameters, such as hydrothermal time, hydrothermal temperature, microwave time, and microwave power, were optimized with quantum yield as the optimization goal. The optical properties of the quantum dots prepared using the two methods were analyzed and characterized by fluorescence spectroscopy and ultraviolet-visible (UV-Vis) absorption spectroscopy. The microstructure and crystallization of CDs were studied using X-ray diffraction (XRD) and transmission electron microscopy (TEM). The structural differences in the quantum dots prepared by these two methods were evaluated using X-ray photoelectron spectroscopy (XPS) and Fourier-transform infrared spectroscopy (FTIR). The effects of different preparation methods on the structural properties of CDs were analyzed. Our findings provide a reference for the further optimization and enhancement of the fluorescence performance of CDs prepared from biomass.

2 Materials And Methods

2.1 Materials

Silver carp scales were purchased from Wuhan Liangzihu Aquatic Processing Co., Ltd. Deionized water was used for all experiments. All reagents used in this study were purchased from Sinopharm Chemical Reagent Company.

2.2 Preparation of CDs

Conventional hydrothermal method: A certain amount of fish scales was weighed, and 25 mL NaOH solution (0.01-0.15 mol/L) was added to completely wet the scales. The mixture was sealed into the hydrothermal reactor and placed in a constant temperature oven (DHG-9140A, Shanghai Yiheng Scientific Instrument, China). After reacting at 170-210℃ for 1-5 h, the mixtures were centrifuged at 12000 rpm for 10 min at room temperature (about 25℃). The supernatant was transferred to a dialysis bag (*MW* cutoff: 1000) and dialyzed against deionized water. The obtained carbon dot sample was identified as CD-HT.

Microwave method: A process similar to that used for the hydrothermal method was employed, with the differences being that the fish scales and NaOH solution were taken in a microwave digestion tank and placed in a microwave reactor (MCR-3, Gongyi Yuhua Instrument, China), and reacted at 80-720 W for a certain time (1-3 min). The purification method was similar to that described above. The obtained carbon dot sample was identified as CD-MW.

A certain amount of the above sample solution was analyzed using UV-absorption and fluorescence spectroscopy, and the freeze-dried samples were used for structural analysis.

2.3 Characterization of CDs

The UV-vis absorption of the aqueous solution of CDs was recorded using a UV-2800 UV-vis spectrophotometer (Unico Instruments, China). Photoluminescence emission measurements were recorded using fluorescence spectroscopy (F98; Lengguang Technology, China). The quantum yield of CDs was calculated using quinine sulfate (quantum yield of 0.54) in 0.1 mol/L H_2SO_4 as the standard. (Guo et al. 2020)

TEM images were acquired using Tecnai G2 F20 (FEI, Netherlands) at an accelerating voltage of 100 kV. The crystal structure of CDs was determined using XRD-7000 (Shimadzu, Japan) under CuKα X radiation. The elemental composition and valence states were determined by XPS using an EscaLab 250Xi (Thermo Scientific, USA). The surface groups of CDs were determined using FTIR (NEXUS, Thermo Nicolet, USA) using KBr pelleting.

2.4 Statistical analysis

Data are expressed as the mean standard deviation and were subjected to analysis of variance, followed by Duncan's multiple range test. Statistically significant differences between different groups of data are indicated with different letters (adjusted $P<0.05$).

3 Results And Discussion

3.1 Optimization of the crushing method of CDs

Fish scales were cleaned and dried to obtain the precursor, and the effects of different crushing methods of fish scales on the quantum yield of CDs were investigated. The quantum yield of CDs prepared using

the conventional hydrothermal method of freeze-grinding fish-scale powder (6.05 ± 0.05%) was significantly higher than that obtained using the conventional ball grinding method (3.87 ± 0.05%) and shearing of fish scales (3.26 ± 0.06%). The macroscopic structure of fish scales obtained using the three different crushing methods was observed using a stereo microscope (**Figure S1**). Compared with the sheared fish-scale powder, the ground (conventional ball grinding, freeze-grinding) fish-scale powder had smaller particles, larger specific surface area, and larger contact area with the dispersion system, which will make CD synthesis more facile and efficient. The fish-scale powder obtained by freeze-grinding was finer, more uniform, and more dispersible than that obtained using conventional ball milling, as the fish scales frozen in liquid nitrogen were more brittle and more easily fractured during the freeze-grinding process.(Lu et al. 2020, Xia et al. 2022)

3.2 Optimization of the reaction parameters to prepare CDs

CDs were prepared using the freeze-ground fish-scale powder as a precursor, and the conventional hydrothermal and microwave preparation methods were further optimized.

3.2.1 Optimization of reaction parameters for CD-HT

CD-HT was prepared by a carbonization reaction under hydrothermal conditions with fish scales as a precursor. The effects of hydrothermal temperature, hydrothermal time, and NaOH concentration on the quantum yield were studied (**Figure S2**). Based on univariate experiments, NaOH concentration (0.03 mol/L, 0.05 mol/L, 0.1 mol/L), hydrothermal temperature (180℃, 190℃, 200℃), and hydrothermal time (2 h, 3 h, 4 h) were selected and analyzed using an orthogonal table $L_9(3^4)$.

The orthogonal experiment was analyzed using range analysis and variance analysis (**Table S1**). Hydrothermal temperature was determined to be the main factor affecting the quantum yield of CDs, followed by NaOH concentration and hydrothermal time. Among the nine trials in the orthogonal test, the preferred combination was determined to be a NaOH concentration of 0.03 mol/L, reaction time of 4 h, and temperature of 200℃. The quantum yield of CD-HT at these conditions was 6.04 ± 0.05%.

3.2.2 Optimization of reaction parameters for CD-MW

Similar to the study performed for CD-HT, the effects of microwave conditions (NaOH concentration, microwave power, microwave time) on the quantum yield of CD-MW were analyzed using single-factor analysis, and the results were shown in **Figure S3**. NaOH concentration (0.01 mol/L, 0.03 mol/L, 0.05 mol/L), microwave power (240 W, 400 W, 560 W), and microwave time (1 min, 1.5 min, 2 min) were selected using the orthogonal table $L_9(3^4)$ for orthogonal experimental analysis.

Results of the orthogonal experiment (**Table S2**) suggested that NaOH concentration with the highest *R*-value had the greatest influence on the fluorescence quantum yield. The influence of the other factors (microwave time and microwave power) on fluorescence quantum yield was secondary. After the verification test, the optimal scheme was as follows: NaOH concentration, 0.01 mol/L; microwave time,

1.5 min; microwave power, 400 W. The quantum yield of CD-MW using these parameters was 5.10 ± 0.13%.

3.3 Optical properties of CDs

The optical properties of the two CD solutions were compared and the results are shown in Fig. 1. The UV-Vis absorption spectra reveal that both CDs have a weak wide absorption band at 250 ~ 290 nm, which may be attributed to the π-π* transition of the C = C bonds during aromatic sp^2 hybridization.(Pandiyan et al. 2020, Reckmeier et al. 2016, Shamsipur et al. 2018) The fluorescence properties of the two CDs were further studied based on their fluorescence spectra. The optimal excitation of CD-HT was 360 nm and the optimal emission was 430 nm, whereas the optimal excitation of CD-MW was 310 nm and optimal emission was 400 nm. The difference was related to the particle size, domain size, and surface states of the CDs.(Ma et al. 2022, Pundi &Chang 2022) The illustrations are images of the two CD solutions visualized using a fluorescent lamp and an ultraviolet lamp. The two CD solutions appeared transparent in visible light and were evenly dispersed without any aggregation or precipitation. Furthermore, they exhibited a bright blue fluorescence under ultraviolet light (365 nm). The fluorescence intensity of CD-HT was stronger than that of CD-MW, which was consistent with their quantum yield.

The fluorescence characteristics of both CDs were analyzed (Fig. 2). When the excitation wavelength of CD-HT increased from 320 nm to 360 nm, the fluorescence intensity increased first and then decreased, and the emission peak redshift was observed. The emission spectra of CD-HT exhibited excitation-related properties, which may be due to the difference in the size of the CDs and the presence of different organic groups on the surface of the CDs that resulted in different surface state distributions.(Khan et al. 2019, Liu et al. 2011) Fluorescence spectrometry of CD-MW revealed that when the excitation wavelength was increased from 280 nm to 350 nm, the corresponding emission positions at different excitation wavelengths were almost unchanged, and a single fixed emission at 400 nm was observed, indicating an almost excitation-independent emission behavior. The nonexcited-state behavior may be because the luminescence properties of CD-MW depend on the surface state rather than the quantum size effect, likely because the amino group enhances the surface functionalization of the carbon surface group, and the surface state of these CD-MW should be fairly uniform.(Karami et al. 2020, Krysmann et al. 2012, Yang et al. 2020)

The stability of the fluorescence performance of CDs is crucial for practical application.(Li et al. 2019, Thulasi et al. 2020, Yun et al. 2022) Therefore, we investigated the stability of both types of CDs under light and ion interference (Fig. 3). The two CDs were continuously excited under a xenon lamp for 120 min to measure their photostability. The luminescence intensity was almost unchanged, indicating the photostability of the prepared CDs. Next, the effect of ionic intensity on the emission spectrum of CDs was determined, and the fluorescence intensities of both CD variants were monitored at different salt concentrations. When the concentration of NaCl was increased from 0.2 mol/L to 1.0 mol/L, the fluorescence intensity was almost unchanged. In addition, both CDs yielded uniformly clarified solutions without obvious precipitation under the interference of salt. This finding showed that both CD variants

had stable fluorescence characteristics at higher salt concentrations. Collectively, our findings revealed that both CD variants exhibited light stability and salt tolerance, which are important characteristics for their practical application.

In summary, both CDs exhibited good light stability and salt tolerance, but their optical properties were different. The excitation was inconsistent (CD-HT excitation at 360 nm and CD-MW excitation at 310 nm); CD-HT exhibited emission behavior related to excitation, whereas CD-MW exhibited emission behavior that was almost independent of excitation. Moreover, the quantum yield of CD-HT was slightly higher than that of CD-MW. This may be closely related to the surface state and also likely affected by the size. Thus, in our subsequent analysis, we will focus on the structural differences between CDs.

3.4 Morphology of CD-HT and CD-MW

The crystal structure of the CDs was analyzed using XRD and the results are shown in Fig. 4. Both CDs showed wide and obvious diffraction peaks, and the diffraction angle was $2\theta = 21.55°$, which, corresponding to the layer spacing d was 0.41 nm. Compared with bulk graphite (about 0.34 nm), the spacing of fluorescent carbon nanoparticles is larger, which may be due to the abundance of O and N groups, resulting in the weak aromatic-layer interaction between the graphite layers.(Rodríguez Padrón et al. 2018, Yang et al. 2018) Therefore, both CDs have the characteristics of amorphous carbon, and the degree of graphitization is low.

The size and structure of CDs were analyzed using TEM (Fig. 5). It can be seen from the TEM diagram that CD-HT is mostly uniform and appears as quasi-spherical nanoparticles with good dispersion. The histogram of size distribution indicated that the particle size-distribution range of CD-HT was 1.7–6.5 nm, average size was 4.02 ± 0.89 nm, and the average diameter was < 5 nm. On the other hand, CD-MW was more inclined to be uneven and appeared as irregular sheets, with a particle size distribution range of 2.4–7.2 nm and an average particle size of 4.23 ± 1.03 nm. The significant differences in morphology between both CD variants may be the main source of their optical properties.

3.5 Surface properties of CD-HT and CD-MW

The chemical structure and state of the elements in the CDs were analyzed using XPS. The XPS full spectrum (**Figure S4**) shows that the prepared CDs contain C, N, O, and Na. A small amount of Na was derived from the residual Na ions during the preparation of CDs. Ca and P were not found in the prepared CDs, indicating no obvious entrainment of these elements into the complex amorphous carbon structure during CD synthesis. This could be attributed to the NaOH system that was used. Under alkaline conditions, the solubility of the main inorganic component, hydroxyapatite, in fish scales was low, resulting in only trace Ca and P ions in the reaction system, which cannot easily participate in CD formation. Elemental composition analysis (Table 1) revealed that the self-doped N element in both CDs was considerable. The passivation effect of the doped elements conferred excellent optoelectronic properties upon the CDs.(Manioudakis et al. 2019) Further improvement showed that there were fewer

doped elements in CD-HT than in CD-MW, which was likely related to the rapid reaction using the microwave method.

Table 1
Surface-element composition of the two CDs

Name	CD-HT	CD-MW
C1s	65.8%	59.4%
N1s	13.1%	16.5%
O1s	21.1%	24.1%

The high-resolution spectra of C_{1s}, N_{1s}, and O_{1s} bands were deconvoluted as shown in Fig. 6. C element exhibited four chemical states at different peak positions: C-C/C = C near 284.8 eV, C-N near 285.9 eV, C-O near 286.5 eV, and C = O near 287.6 eV.(Fang &Zheng 2021) The content of different chemical states calculated by peak area are as follows: for CD-HT, the C-C/C = C content was 59.8%, C-N content was 10.9%, C-O content was 6.5%, and C = O content was 22.9%. For CD-MW, the C-C/C = C content was 39.8%, C-N content was 24.2%, C-O content was 8.5%, and C = O content was 27.3%. CD-HT contained more C-C/C = C, whereas the other three chemical states (structural defects) were less; these findings indicated that the doping of heteroatoms in CD-HT was less, which was consistent with the elemental analysis results of the total spectrum.

In addition to C, the N_{1s} spectrum was fitted into four main peaks (Fig. 6B), which were attributed to pyridine N (398.5 eV), amine N (399.7 eV), pyrrole N (400.2eV) and quaternary N (401.3 eV).(Liu et al. 2020, Pillar-Little &Kim 2017) By analyzing the ratio of the different types of N, we found that CD-HT had a higher proportion of pyrrole N, conferring upon its better charge mobility and donor-acceptor ability, which is beneficial in the improvement of its quantum yield. Moreover, a small amount of oxidized N is present in CD-HT. The O_{1s} spectrum (Fig. 6C) can be deconvoluted into two peaks at 531.1 eV and 532.4 eV, which are attributed to the presence of C = O and C-OH/C-O-C, respectively.(Liu et al. 2020) Oxygen in CD-MW tends to exist in the form of C-OH/C-O-C, whereas oxygen in CD-HT exists in the form of C = O, which is also conducive to the improvement of quantum yield.

The functional groups of CDs were further analyzed using FTIR, and the main signal regions that were identified are shown in Fig. 7.(Dutta 2017) The total spectrum (**Figure S4**) and specific peak parameters are shown in the Supporting Material (**Table S3** and **Table S4**).

In Fig. 7A, the peak at ~ 3560 cm^{-1} represents the O-H stretching vibration of -COOH in CD-HT, which is significantly stronger than that in CD-MW, indicating that CD-HT contains more -COOH, which is consistent with the results from XPS. For the signal peaks representing the N-H stretching vibration at ~ 3450 cm^{-1}, and N-H and O-H stretching vibrations at ~ 3300 cm^{-1}, the peak area of CD-HT is smaller than that of CD-MW, which is related to the less doping of N and O elements in CD-HT. The wider peak

shape of CD-MW was attributed to higher hydrogen bond association, indicating the hydrophilicity of CD-MW. The signal peaks of = C-H and Ar-H (3060 cm^{-1}) and of saturated C-H asymmetric vibration (2860 cm^{-1}, ~ 2960 cm^{-1}, and 2944 cm^{-1}) in CD-HT were significantly stronger than those of CD-MW, which also indicated the high carbonization degree of CD-HT.

As shown in Fig. 7B, the peak area representing the C = C stretching vibration (~ 1650 cm^{-1}) in CD-HT is significantly larger than that in CD-MW, which is consistent with previous XPS results. There is no significant difference between the signal of N-H bending vibration and C-N stretching vibration of the amide at ~ 1560 cm^{-1}. The signal at ~ 1520 cm^{-1} attributed to the asymmetric stretching vibration of -NO_2 in CD-HT is significantly higher than that in CD-MW, indicating higher -NO_2 content. The peaks in the range of 1480 ~ 1350 cm^{-1} are mainly attributed to C-H bending vibration in -CH_3/-CH_2-; the corresponding signal peaks in CD-HT are more obvious, indicating a higher number of C-H bonds, which are closely related to its higher degree of carbonization. Additionally, the signal peak (1420 cm^{-1}) of C-O stretching vibration and O-H bending vibration in CD-HT attributed to -COOH is stronger than that in CD-MW, which is consistent with the analysis results of -COOH (Fig. 7A**)**.

The above analyses revealed that due to the different heating methods used, CDs prepared from fish scales using the conventional hydrothermal and microwave methods exhibited obvious differences in optical properties, structural morphology, and surface group composition (Fig. 8**)**.

Microwave heating can rapidly and uniformly increase the temperature of the reaction system and promote the carbonization of organic matter (mainly collagen) in fish scales to form CDs. The result of the rapid reaction is that the abundant N (~ 17%) in the organic matter is carried and doped into the product CDs to a greater extent, resulting in CDs with higher N doping. On the other hand, the slow heating using the conventional hydrothermal method was helpful in obtaining a more balanced product with lower local energy. Thus, N doping in CD-HT was less, but a relatively large proportion in the form of pyrrole N was present and a certain amount of -NO_2 was formed.

Microwave heating puts forth higher requirements for reaction vessels. The use of traditional stainless steel sealed reaction vessels is limited, whereas conventional PTFE or glass containers cannot provide effective sealing strength. Thus, the temperature of the reaction system is usually only slightly > 100°C. Therefore, only a part of the protein (mainly collagen) could dissolve to form the nanosheet-like fluorescent material. TGA analysis of the precipitate in the reaction system of the microwave method showed a large amount of organic matter (**Figure S5**). In contrast, the heating temperature of the hydrothermal reaction has no obvious restrictions and can be preset to temperatures > 100°C. Therefore, CDs with higher carbonization degree, smaller size, and higher C = O/COOH content were obtained. These structural features are the main reasons for the higher quantum yield and lower excitation wavelength of CD-HT.

4 Conclusions

The effects of conventional hydrothermal and microwave methods on the fluorescence performance and structure of CDs were investigated using fish scales as a precursor. Both CD variants prepared under optimal conditions were characterized and compared. Both CDs exhibited blue fluorescence under ultraviolet light and had good dispersion, light stability, and salt tolerance. The rapid and uniform microwave heating method was more conducive to the self-doping of N. However, owing to the sealing limitations of the reaction vessel, the low temperature of the microwave method leads to incomplete dissolution of the organic matter in fish scales; moreover, the dissolved organic matter is more difficult to completely dehydrate and condense. Thus, nanosheet-like fluorescent CDs are formed wherein the emission behavior has no significant correlation with excitation. Although the N doping of CDs prepared using the conventional hydrothermal is low, the relative pyrrolic N content is high, which is beneficial in improving quantum yield. Additionally, the controllable high temperature and sealed environment of the conventional hydrothermal method can promote the dehydration and condensation of organic matter in fish scales to form CDs with a higher degree of carbonization, uniform size, and higher C = O/COOH content, as well as higher quantum yield and excitation wavelength-related emission behavior. These will provide guidance for the structural optimization and practical use of biomass-derived carbon dots.

Declarations

Funding: This work was supported by the National Natural Science Foundation of China (Grant numbers 22178277), the Hubei Provincial Key Laboratory of Occurrence and Intervention of Rheumatic Diseases (Grant numbers PT022205).

Competing Interests: The authors have no relevant financial or non-financial interests to disclose.

Author Contributions: All authors contributed to the study conception and design. Material preparation, data collection and analysis were performed by Chengzhi Xu, Xiao Xiao, Chaonan Cai, Qunpeng Cheng, Lian Zhu, Juntao Zhang and Benmei Wei. The first draft of the manuscript was written by Chengzhi Xu and Haibo Wang. All authors commented on previous versions of the manuscript. All authors read and approved the final manuscript.

Ethical Approval: Not applicable.

Consent to Participate: Not applicable.

Consent to Publish: Not applicable.

Availability of Data and Materials: Data will be made available upon request.

Acknowledgements

The authors would like to thank all the reviewers who participated in the review.

References

1. Ashraf PM, Stephen S, Binsi PK (2021): Sustainable process to co-synthesize nano carbon dots, nano hydroxyapatite and nano β-dicalcium diphosphate from the fish scale. Applied Nanoscience 11, 1929-1947
2. Athinarayanan J, Periasamy VS, Alshatwi AA (2020): Simultaneous fabrication of carbon nanodots and hydroxyapatite nanoparticles from fish scale for biomedical applications. Materials Science and Engineering: C 117, 111313
3. Campalani C, Cattaruzza E, Zorzi S, Vomiero A, You S, Matthews L, Capron M, Mondelli C, Selva M, Perosa A (2021): Biobased Carbon Dots: From Fish Scales to Photocatalysis. Nanomaterials 11, 524
4. Chen Q-L, Ji W-Q, Chen S (2016): Direct Synthesis of Multicolor Fluorescent Hollow Carbon Spheres Encapsulating Enriched Carbon Dots. Sci. Rep. 6, 19382
5. Deb P, Barua E, Deoghare AB, Lala SD (2019): Development of bone scaffold using Puntius conchonius fish scale derived hydroxyapatite: Physico-mechanical and bioactivity evaluations. Ceram. Int. 45, 10004-10012
6. Dhandapani E, Duraisamy N, Periasamy P, T PV (2020): Highly green fluorescent carbon quantum dots synthesis via hydrothermal method from fish scale. Mater. Today:. Proc. 26, A1-A5
7. Dutta A (2017): Chapter 4 - Fourier Transform Infrared Spectroscopy. In: Thomas S, Thomas R, Zachariah AK , Mishra RK (Editors), Spectroscopic Methods for Nanomaterials Characterization. Elsevier, pp. 73-93
8. Fang L, Zheng J (2021): Carbon quantum dots: Synthesis and correlation of luminescence behavior with microstructure. New Carbon Mater. 36, 625-631
9. Ghanem A, Al-Qassar Bani Al-Marjeh R, Atassi Y (2020): Novel nitrogen-doped carbon dots prepared under microwave-irradiation for highly sensitive detection of mercury ions. Heliyon 6, e03750
10. Golden CD et al. (2021): Aquatic foods to nourish nations. Nature 598, 315-320
11. Guo F, Zhu Z, Zheng Z, Jin Y, Di X, Xu Z, Guan H (2020): Facile synthesis of highly efficient fluorescent carbon dots for tetracycline detection. Environ. Sci. Pollut. Res. 27, 4520-4527
12. Karami S, Shamsipur M, Taherpour AA, Jamshidi M, Barati A (2020): In Situ Chromophore Doping: A New Mechanism for the Long-Wavelength Emission of Carbon Dots. J. Phys. Chem. C 124, 10638-10646
13. Khan ZMSH, Rahman RS, Shumaila, Islam S, Zulfequar M (2019): Hydrothermal treatment of red lentils for the synthesis of fluorescent carbon quantum dots and its application for sensing Fe3+. Opt. Mater. 91, 386-395
14. Krishnani KK, Boddu VM, Chadha NK, Chakraborty P, Kumar J, Krishna G, Pathak H (2022): Metallic and non-metallic nanoparticles from plant, animal, and fisheries wastes: potential and valorization for application in agriculture. Environ. Sci. Pollut. Res. 29, 81130-81165
15. Krysmann MJ, Kelarakis A, Dallas P, Giannelis EP (2012): Formation Mechanism of Carbogenic Nanoparticles with Dual Photoluminescence Emission. J. Am. Chem. Soc. 134, 747-750

16. Lee TC, Mohd Pu'ad NAS, Alipal J, Muhamad MS, Basri H, Idris MI, Abdullah HZ (2022): Tilapia wastes to valuable materials: A brief review of biomedical, wastewater treatment, and biofuel applications. Mater. Today:. Proc. 57, 1389-1395
17. Li J, Cao L, Li D, Yu C, Tan M (2019): Carbon dots from roasted mackerel (scomberomorus niphonius) for free radical scavenging. LWT 111, 588-593
18. Liu S, Tian J, Wang L, Luo Y, Zhai J, Sun X (2011): Preparation of photoluminescent carbon nitride dots from CCl_4 and 1,2-ethylenediamine: a heat-treatment-based strategy. J. Mater. Chem. 21, 11726-11729
19. Liu Y, Zhu C, Gao Y, Yang L, Xu J, Zhang X, Lu C, Wang Y, Zhu Y (2020): Biomass-derived nitrogen self-doped carbon dots via a simple one-pot method: Physicochemical, structural, and luminescence properties. Appl. Surf. Sci. 510, 145437
20. Lu Z, Xie T, Chen H, Li L, Li S, Lu Y, Hu X (2020): Evaluation of effects of freezing pretreatment on the grindability, energy consumption and chemical composition of wheat straw. Renewable Energy 151, 21-29
21. Luo J, Zhou Z, Yao X, Fu Y (2020): Mineral-chelating peptides derived from fish collagen: Preparation, bioactivity and bioavailability. LWT 134, 110209
22. Ma P, Zuo J, Li Z, Xiao D, Wu H, Zhang Y, Dong A (2022): Application Progress of Green Carbon Dots in Analysis and Detection. Particle & Particle Systems Characterization 39, 2200104
23. Manioudakis J, Victoria F, Thompson CA, Brown L, Movsum M, Lucifero R, Naccache R (2019): Effects of nitrogen-doping on the photophysical properties of carbon dots. J. Mater. Chem. C 7, 853-862
24. Niu J, Shao R, Liu M, Zan Y, Dou M, Liu J, Zhang Z, Huang Y, Wang F (2019): Porous Carbons Derived from Collagen-Enriched Biomass: Tailored Design, Synthesis, and Application in Electrochemical Energy Storage and Conversion. Adv. Funct. Mater. 29, 1905095
25. Pandiyan S, Arumugam L, Srirengan SP, Pitchan R, Sevugan P, Kannan K, Pitchan G, Hegde TA, Gandhirajan V (2020): Biocompatible Carbon Quantum Dots Derived from Sugarcane Industrial Wastes for Effective Nonlinear Optical Behavior and Antimicrobial Activity Applications. ACS Omega 5, 30363-30372
26. Pillar-Little T, Kim DY (2017): Differentiating the impact of nitrogen chemical states on optical properties of nitrogen-doped graphene quantum dots. RSC Adv. 7, 48263-48267
27. Pundi A, Chang CJ (2022): Recent Advances in Synthesis, Modification, Characterization, and Applications of Carbon Dots. Polymers 14, 2153
28. Reckmeier CJ, Wang Y, Zboril R, Rogach AL (2016): Influence of Doping and Temperature on Solvatochromic Shifts in Optical Spectra of Carbon Dots. J. Phys. Chem. C 120, 10591-10604
29. Rodrigues DP, Calado R, Ameixa OMCC, Valcarcel J, Vázquez JA (2021): Valorisation of Atlantic codfish (Gadus morhua) frames from the cure-salting industry as fish protein hydrolysates with in vitro bioactive properties. LWT 149, 111840

30. Rodríguez Padrón D, Algarra M, Tarelho LAC, Frade J, Franco A, de Miguel G, Jiménez J, Rodríguez Castellón E, Luque R (2018): Catalyzed Microwave-Assisted Preparation of Carbon Quantum Dots from Lignocellulosic Residues. ACS Sustainable Chem. Eng. 6, 7200-7205
31. Shamsipur M, Barati A, Taherpour AA, Jamshidi M (2018): Resolving the Multiple Emission Centers in Carbon Dots: From Fluorophore Molecular States to Aromatic Domain States and Carbon-Core States. J. Phys. Chem. Lett. 9, 4189-4198
32. Sharma V, Tiwari P, Mobin SM (2017): Sustainable carbon-dots: recent advances in green carbon dots for sensing and bioimaging. J. Mater. Chem. B 5, 8904-8924
33. Sierra L, Fan H, Zapata J, Wu J (2021): Antioxidant peptides derived from hydrolysates of red tilapia (Oreochromis sp.) scale. LWT 146, 111631
34. Thulasi S, Kathiravan A, Asha Jhonsi M (2020): Fluorescent Carbon Dots Derived from Vehicle Exhaust Soot and Sensing of Tartrazine in Soft Drinks. ACS Omega 5, 7025-7031
35. Xia L, Wei X, Wang H, Ye F, Liu Z (2022): Valuable metal recovery from waste tantalum capacitors via cryogenic crushing-alkaline calcination-leaching process. J. Mater. Res. Technol. 16, 1637-1646
36. Xin Y, Odachi K, Shirai T (2022): Fabrication of ultra-bright carbon nano-onions via a one-step microwave pyrolysis of fish scale waste in seconds. Green Chem. 24, 3969-3976
37. Yang P, Zhu Z, Zhang W, Zhang T, Li X, Luo M, Chen W, Chen M, Zhou X (2020): Fluorescence mechanism of xylan-derived carbon dots: Toward investigation on excitation-related emission behaviors. J. Lumin. 223, 117199
38. Yang Q, Duan J, Yang W, Li X, Mo J, Yang P, Tang Q (2018): Nitrogen-doped carbon quantum dots from biomass via simple one-pot method and exploration of their application. Appl. Surf. Sci. 434, 1079-1085
39. Yao QF, Zhou DS, Yang JH, Huang WT (2020): Directly reusing waste fish scales for facile, large-scale and green extraction of fluorescent carbon nanoparticles and their application in sensing of ferric ions. Sustainable Chemistry and Pharmacy 17, 100305
40. Yun S, Kang ES, Choi JS (2022): Zn-assisted modification of the chemical structure of N-doped carbon dots and their enhanced quantum yield and photostability. Nanoscale Advances 4, 2029-2035
41. Zhang Y, Gao Z, Zhang W, Wang W, Chang J, Kai J (2018): Fluorescent carbon dots as nanoprobe for determination of lidocaine hydrochloride. Sens. Actuators, B 262, 928-937
42. Zhang Y, Gao Z, Yang X, Chang J, Liu Z, Jiang K (2019): Fish-scale-derived carbon dots as efficient fluorescent nanoprobes for detection of ferric ions. RSC Adv. 9, 940-949
43. Zhao C, Li X, Cheng C, Yang Y (2019): Green and microwave-assisted synthesis of carbon dots and application for visual detection of cobalt(II) ions and pH sensing. Microchem. J. 147, 183-190

Figures

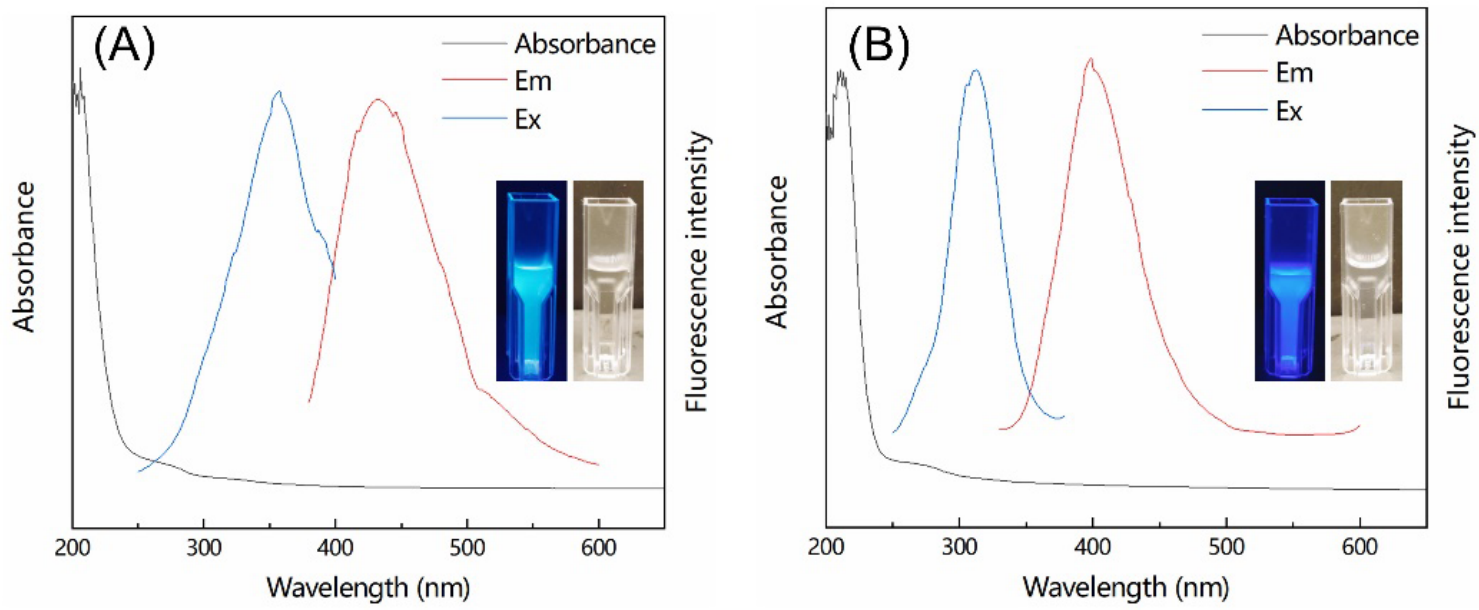

Figure 1

UV and fluorescence spectra of CDs (illustrated as pictures visualized using UV and fluorescent lamps), (A) CD-HT; (B) CD-MW

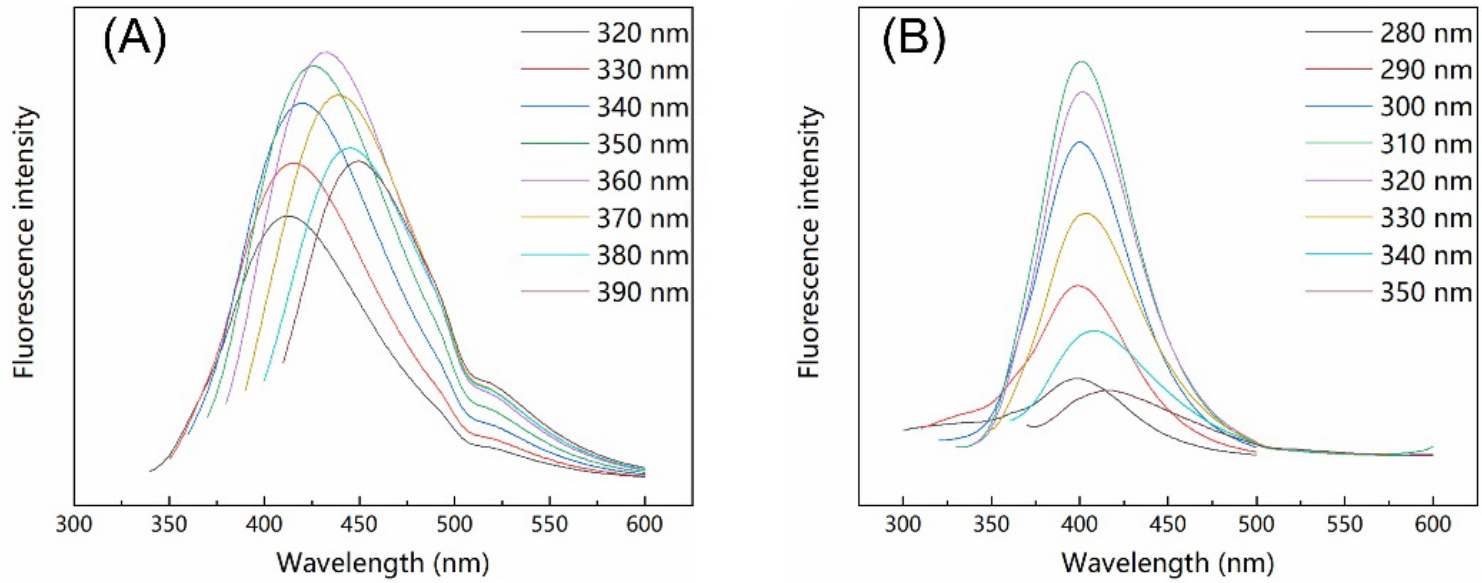

Figure 2

Fluorescence spectra of CDs at different excitation wavelengths, (A) CD-HT; (B) CD-MW

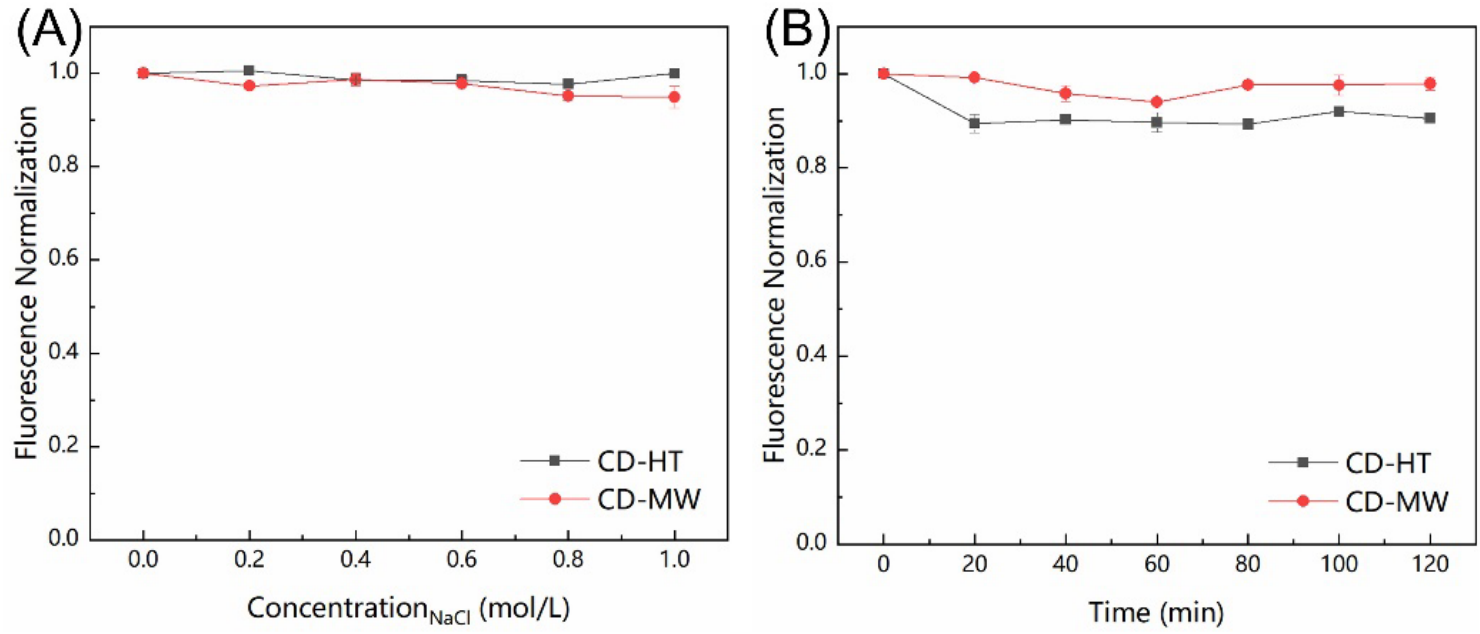

Figure 3

Effects of xenon lamp irradiation time (A) and ionic intensity (B) on the fluorescence intensity of CDs

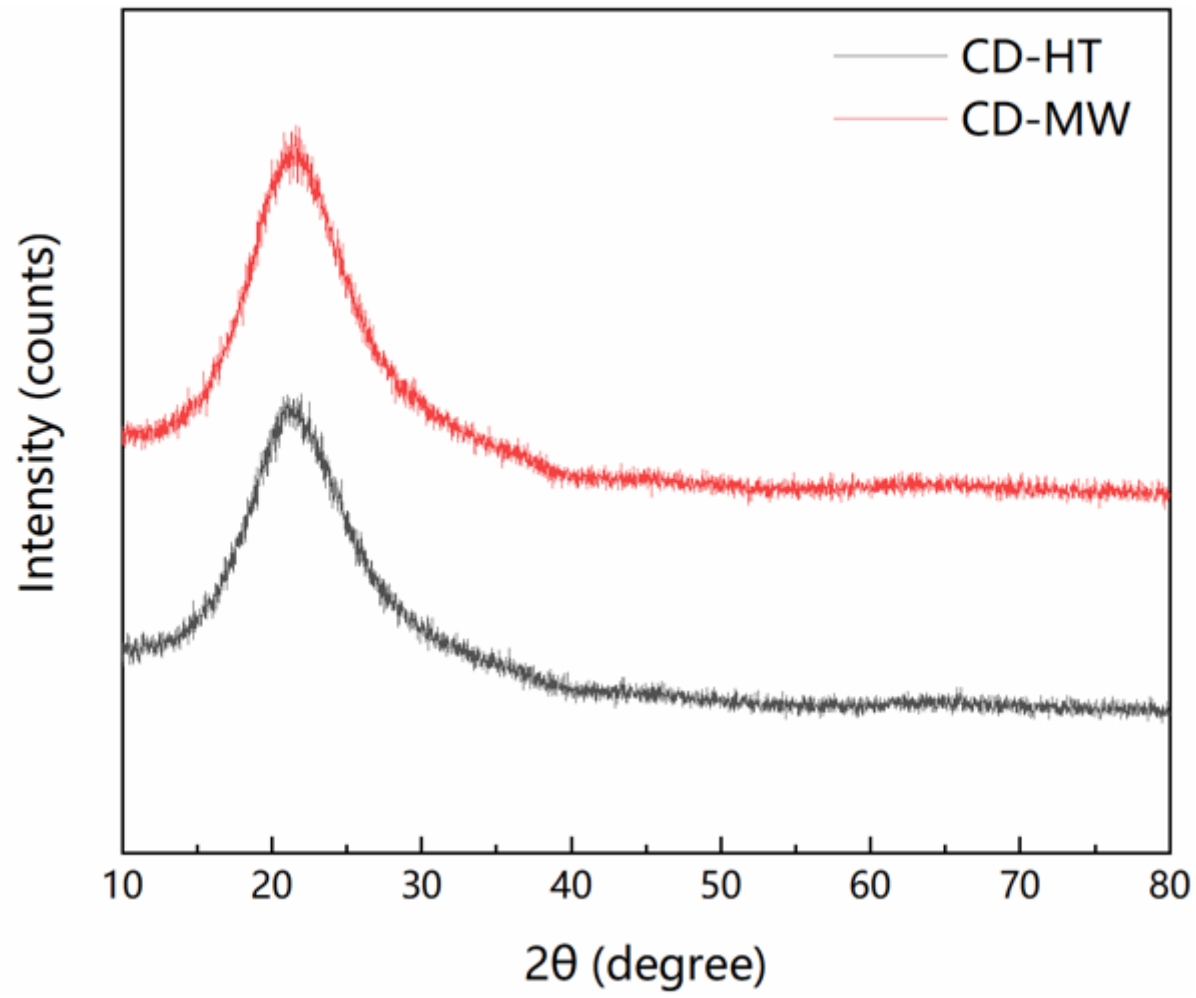

Figure 4

XRD characterization of CDs prepared using conventional hydrothermal (CD-HT) and microwave (CD-MW) methods

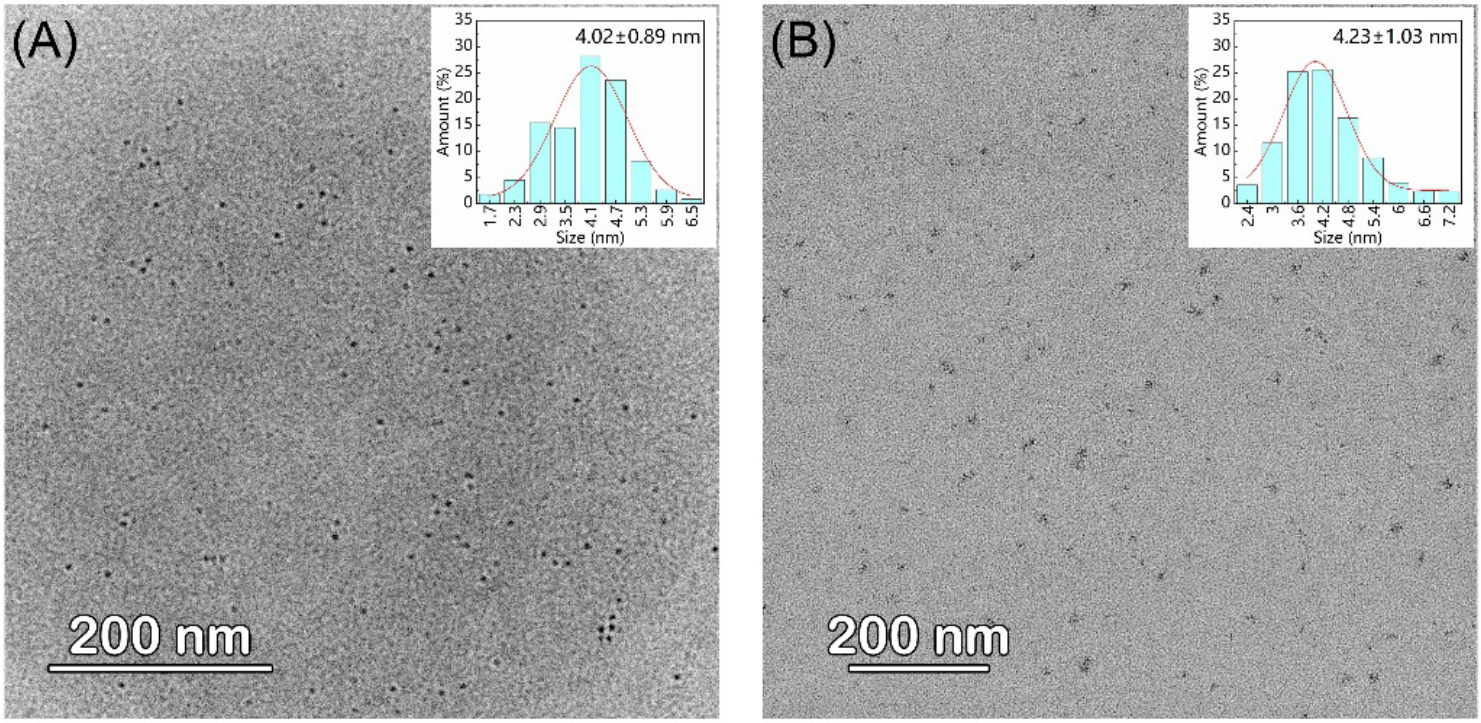

Figure 5

TEM image and particle size distribution of CD-HT and CD-MW

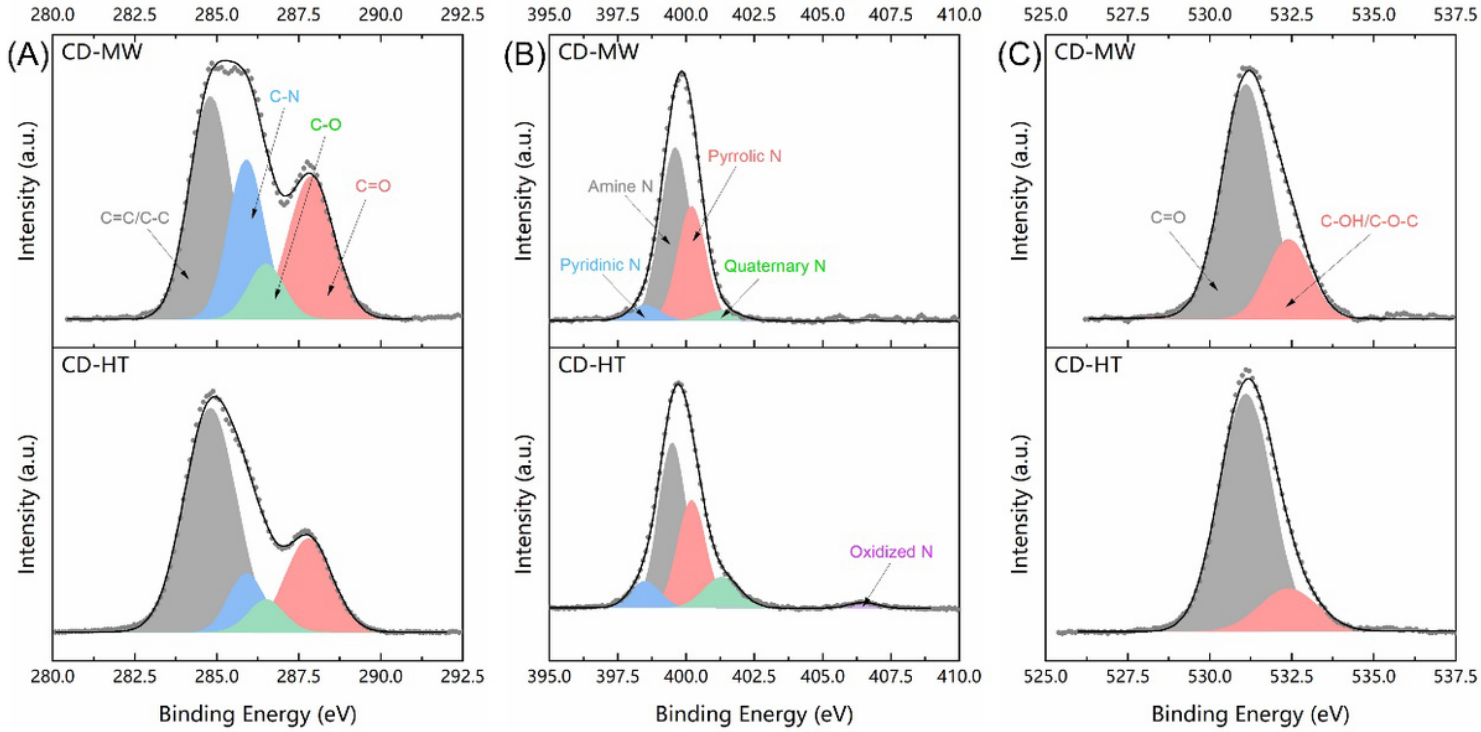

Figure 6

High-resolution XPS of C_{1s} (A), N_{1s} (B), and O_{1s} (C)

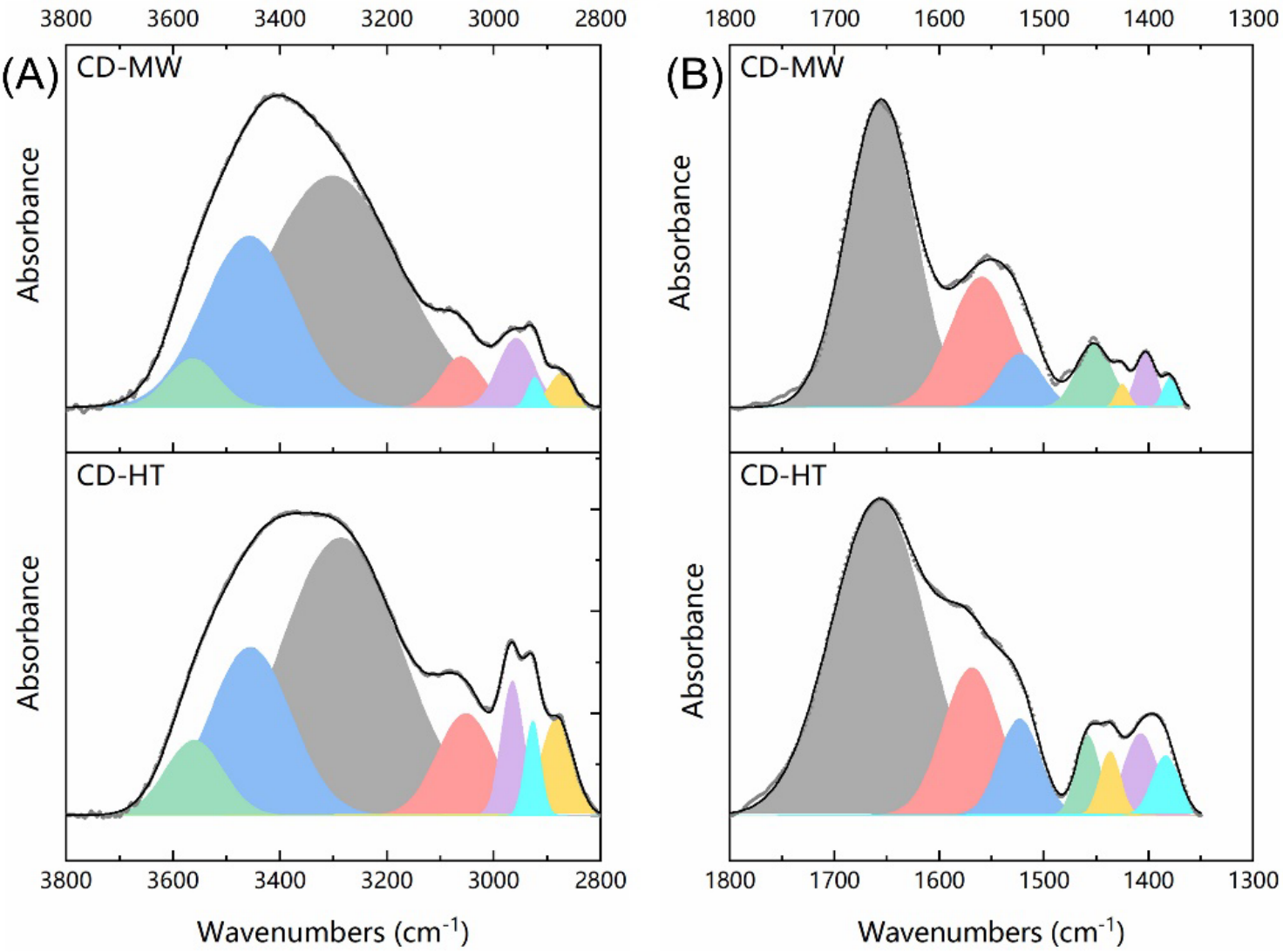

Figure 7

Infrared spectra of CD-HT and CD-MW

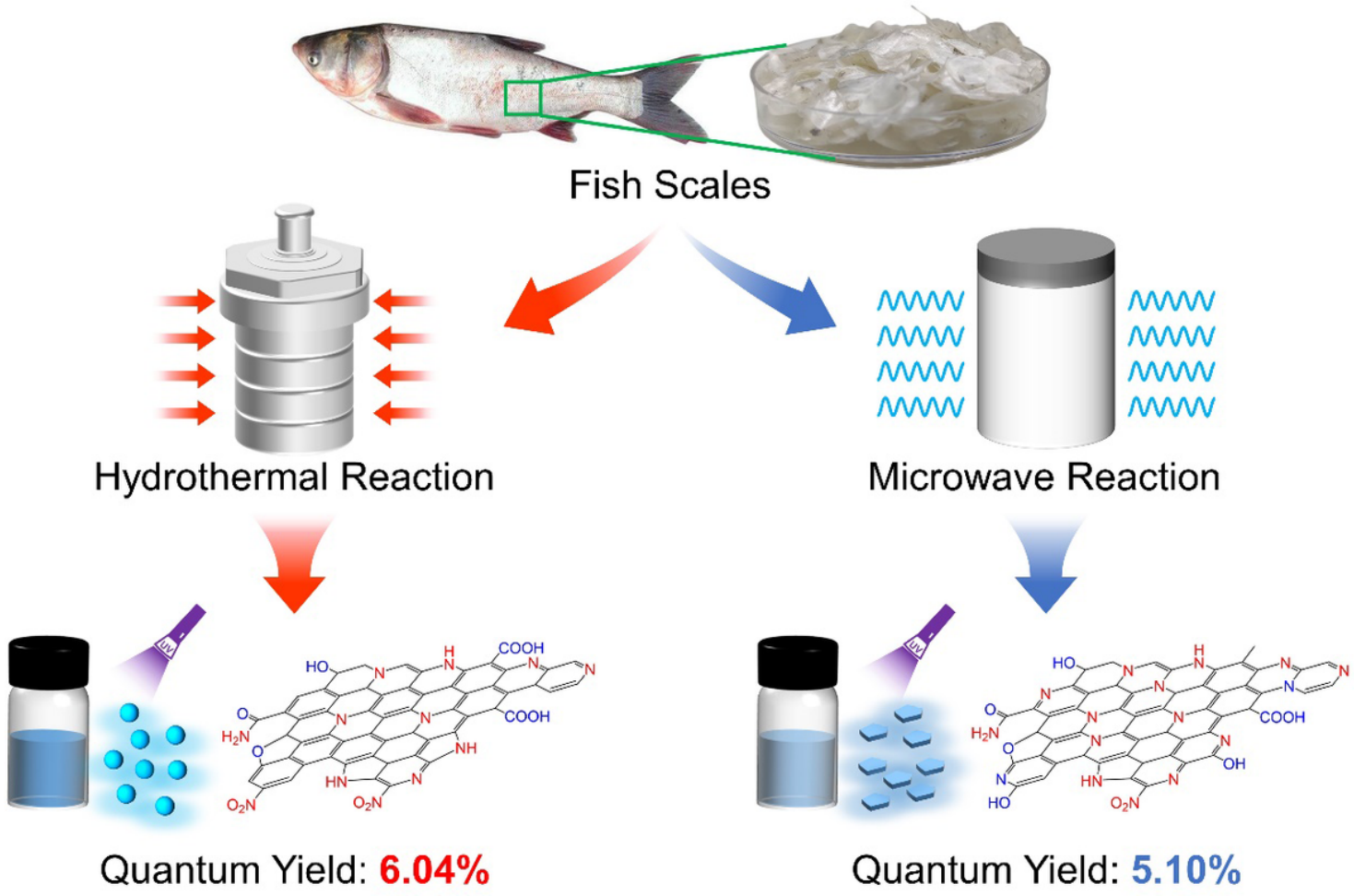

Figure 8

Diagram showing differences in CDs prepared using the hydrothermal and microwave methods

Supplementary Files

This is a list of supplementary files associated with this preprint. Click to download.

- SupplementaryMaterial.docx